23rd International Congress on Sound & Vibration
Athens, Greece 10-14 July 2016
ICSV23

EFFICIENT CALCULATION OF THERMOACOUSTIC MODES UTILIZING STATE-SPACE MODELS

Max Meindl, Thomas Emmert and Wolfgang Polifke
Technische Universität München, Professur für Thermofluiddynamik, 85747 Garching, Germany
email: meindl@tfd.mw.tum.de

This paper describes a framework for the efficient computation of thermoacoustic modes in annular combustors. It is based on state-space models for coupling both the linearized acoustics and the flame dynamics. The state space models for the acoustics are exported from COMSOL Multiphysics. The Finite Element Method for the linearized Euler equations yields very sparse system matrices. The acoustic and the flame models are connected by network model routines. Due to the state-space modeling, thermoacoustic modes can be computed by solving a generalized non-Hermitian linear eigenvalue problem instead of a nonlinear eigenvalue problem. The Arnoldi algorithm is used to calculate selected eigenvalues in case the systems are too big to compute a direct solution for all the eigenvalues. Validation is carried out for a plenum-burner-chamber configuration with four burners. Simplistic n-τ models are chosen for the flame-acoustic interaction, which are represented in state space form utilizing an advection equation for representing the time delay. The results show good agreement with a full three-dimensional Finite Volume Helmholtz solver in mode shape, frequency and growth rates. Coupling between the plenum and the chamber is observed to be dependent on the interaction index and the characteristic time delay of the flame models.

1. Introduction

Premixed flames in gas turbines are widely used, since they feature high efficiency paired with low emissions. However, they are susceptible to self excited thermoacoustic instabilities, which occur due to interactions between fluctuating heat release of the flame and acoustic waves. These waves are reflected by the combustion chamber walls. In the design stage, analytical and numerical methods can be used to predict the stability of a gas turbine. Compressible LES simulations are very expensive and thus low-order models are often utilized to predict stability. So called network models have become very popular, in which the acoustic behavior and the flame-acoustic coupling are captured in modular blocks, which can be connected to build a complete thermoacoustic system [1]. Though being very affordable, low-order models are mostly limited to quasi 1-D wave propagation [2], which often assumes azimuthal compactness of annular geometries. Models for more complex geometries are based on a modal reduction technique [3, 4]. The latter procedure requires a priori knowledge of the system, because the modal basis strongly influences the behavior of the deduced model.

A different approach to thermoacoustic stability is the calculation of the system eigenmodes on a perturbation equation for describing the acoustics (e.g. Helmholtz [5] or linearized Navier-Stokes [6] equations). The flame's response to acoustic fluctuations is typically accounted for by the frequency response of a flame transfer function (FTF). Then the eigenvalue problem needs to be solved iteratively due to the nonlinear coupling of the FTF, which again leads to high computational cost.

In this paper, a method for the efficient stability analysis of gas turbine combustion chambers is introduced, which is based on state-space models for both the acoustic and the flame response. No

a priori knowledge of the system acoustics is required, because the acoustic is only based on the governing equations deduced from first principles instead of a modal reduction.

The paper is organized as follows: Section 2 shows the methods for acquiring state-space models for the acoustic and the FTF, section 3 outlines the validation case setup. In section 4, the results for the validation case are presented. Section 5 concludes with a discussion and provides an outlook on the potential of this method.

2. State-Space Models

State-Space Models are a compact and efficient way to represent a set of linear coupled differential equations. The state vector $\mathbf{x}$ contains the states retained to represent the system. Matrix $\mathbf{A}$ and $\mathbf{E}$ describe the full dynamic of the system and $\mathbf{B}$ models the effect of the inputs $\mathbf{u}$, see Eq. (1). Equation (2) defines an output-vector $\mathbf{y}$, which is a linear combination of the states and the inputs, determined by the output-matrix $\mathbf{C}$ and the feedthrough-matrix $\mathbf{D}$.

$$\mathbf{E}\frac{d\mathbf{x}}{dt} = \mathbf{A}\mathbf{x} + \mathbf{B}\mathbf{u} \tag{1}$$

$$\mathbf{y} = \mathbf{C}\mathbf{x} + \mathbf{D}\mathbf{u} \tag{2}$$

Time domain simulation is straight forward by discretization of the time derivative of $\mathbf{x}$. From the Laplace-transfomred system, the in-/output transfer functions as well as the eigenvalues can be calculated.

2.1 Acoustic state-space model

In this study, the linearized Euler equations (LEE) are employed for the acoustic modeling [7]. Only the source term $\dot{q}'_v$ for the unsteady heat release in the linearized conservation of energy, Eq. (5), is kept.

$$\frac{\partial \rho'}{\partial t} + \nabla\rho' \cdot \bar{\mathbf{u}} + \rho'\nabla \cdot \bar{\mathbf{u}} + \nabla\bar{\rho} \cdot \mathbf{u}' + \bar{\rho}\nabla \cdot \mathbf{u}' = 0 \tag{3}$$

$$\bar{\rho}\frac{\partial \mathbf{u}'}{\partial t} + \bar{\rho}(\bar{\mathbf{u}} \cdot \nabla)\mathbf{u}' + \bar{\rho}(\mathbf{u}' \cdot \nabla)\bar{\mathbf{u}} + \rho'(\bar{\mathbf{u}} \cdot \nabla)\bar{\mathbf{u}} + \nabla p' = 0 \tag{4}$$

$$\frac{\partial p'}{\partial t} + \bar{\mathbf{u}} \cdot \nabla p' + \mathbf{u}' \cdot \nabla\bar{p} + \gamma(\bar{p}\nabla \cdot \mathbf{u}' + p'\nabla \cdot \bar{\mathbf{u}}) = (\gamma - 1)\dot{q}'_v \tag{5}$$

Here, $\bar{(\cdot)}$ are the mean values and $(\cdot)'$ are the acoustic perturbations. Equations (3) - (5) are spatially discretized using a Finite Element Method (FEM). Together with boundary conditions, a linear set of equations results from the FEM.

$$\mathbf{E}\frac{d\mathbf{x}}{dt} + \mathbf{K}\mathbf{x} = \mathbf{L} \tag{6}$$

Here, $\mathbf{E}$ is the mass matrix, $\mathbf{K}$ is the stiffness matrix and the load vector $\mathbf{L}$ contains entries which originate from Dirichlet boundary conditions and source terms. The state-vector $\mathbf{x}$ contains the acoustic variables at all spatial discretization points, which have not been eliminated by boundary conditions. The length N_A of the state vector equals the degrees of freedom of the acoustic system.

Equation (6) can be transformed to state-space representation by choosing $\mathbf{A} = -\mathbf{K}$ and splitting the load vector in two factors, a matrix $\mathbf{B}$ with constant coefficients and a vector $\mathbf{u}$ which contains the time dependent input signals, e.g. unsteady heat release. By means of the output matrix $\mathbf{C}$, the user can define output variables which are linear combinations of the states. These outputs can be chosen arbitrarily as they do not effect the dynamics of the system.

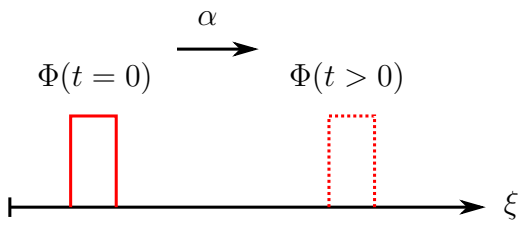

Figure 1: Illustration of a signal Φ being advected along ξ.

2.2 Flame state-space model

A flame transfer function with a single time-lag, e.g. the $n-\tau$ model, represents a flame that reacts to an acoustic perturbation after a time-lag τ. A linear model for the time-lag, which is the crucial part of the $n-\tau$ model, can be derived e.g. by means of a Padé-approximation ([1]). For increasing τ however, the Padé-approximation requires an increased number of coefficients which become ill conditioned. The approach taken in this paper is the utilization of the 1D advection differential equation to model the time-lag.

$$\frac{\partial \Phi}{\partial t} + \alpha \frac{\partial \Phi}{\partial \xi} = 0 \tag{7}$$

In Eq. (7), the property Φ is transported with the constant advection speed $\alpha > 0$ in positive ξ direction (compare Fig. 1). Assume an advection along a fixed interval of length T in ξ direction. Subsequently, the time τ it takes for a signal Φ to be transported is $\tau = T/\alpha$.

For the $n-\tau$ model, a signal Φ is imposed at the upstream boundary ($\xi = 0$). At the downstream boundary ($\xi = T$), the time-lagged signal is measured and amplified by the factor n.

To obtain the state-space form, the interval T is discretized in $N_F - 1$ elements of size ΔT by means of an upwind difference scheme which yields N_F degrees of freedom. The input signal to this model is the acoustic velocity perturbation u' at a reference position, the measured output $\dot{q}'_V$ is the time delayed input signal, amplified by the flame-gain n. The states correspond to the advected property at the respective discretization nodes between the elements. Equations (8) and (9) illustrate a state-space model with $N_F = 4$ degrees of freedom, discretized with a first order upwind scheme. The input acts only on the first state (upstream boundary), whereas the output vector $\mathbf{C}$ uses the last state only (downstream boundary). For this case, the coefficients in $\mathbf{A}$ and $\mathbf{B}$ are $a = \alpha/\Delta T$.

$$\frac{d\mathbf{x}}{dt} = \underbrace{\begin{bmatrix} -a & 0 & 0 & 0 \\ a & -a & 0 & 0 \\ 0 & a & -a & 0 \\ 0 & 0 & a & -a \end{bmatrix}}_{\mathbf{A}} \mathbf{x} + \underbrace{\begin{bmatrix} a \\ 0 \\ 0 \\ 0 \end{bmatrix}}_{\mathbf{B}} u' \tag{8}$$

$$\dot{q}'_V = \underbrace{\begin{bmatrix} 0 & 0 & 0 & n \end{bmatrix}}_{\mathbf{C}} \mathbf{x} \tag{9}$$

By modeling the time-lag with an advection equation, a well conditioned, linear system in time-domain results. Using higher order upwind schemes or more discretization points increases the accuracy of the model for higher frequencies. Figure 2 (left) shows the step responses for two models of order $N_F = 100$ and $N_F = 30$, both discretized with a third order upwind scheme. Slight under- and overshoots are observed close to the step. The higher order model has a steeper response, whereas the overshoot amplitude remains constant. However, for harmonic excitations, which are important in acoustics, the model performs excellent up to a certain frequency, which depends on the model order (Figure 2 (right)). As intended, the gain remains at a constant value of 1 up to a certain frequency, while the phase decreases linearly, which implies a constant time-lag.

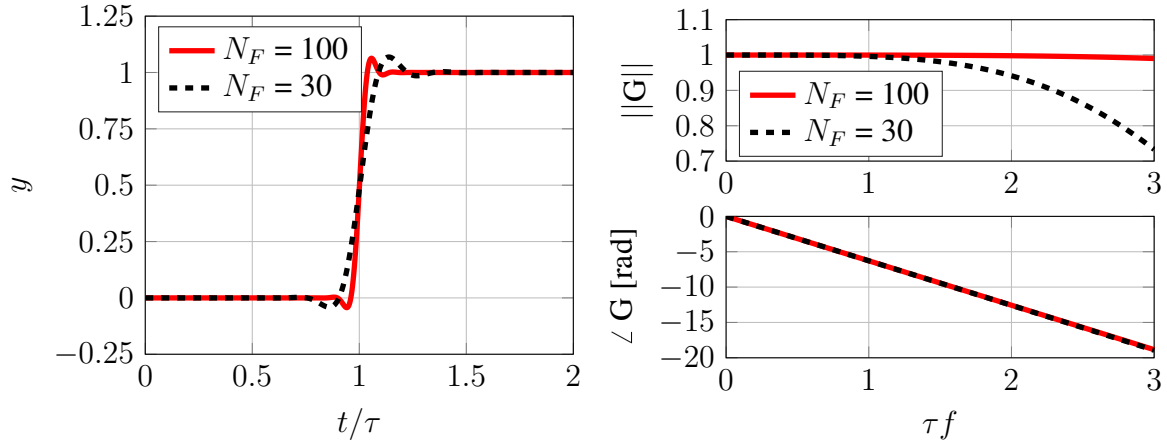

Figure 2: Step response (left) and transfer function $G(\omega)$ (right) of a $n - \tau$ state-space model, $\tau = 1$ ms, $n = 1$.

The implementation of a linear FTF with multiple time-delays, which is the more accurate and generic way to describe the flame-acoustic interaction, is also straightforward ([8]). This allows for incorporation of FTFs which were measured from experiments or identified from CFD simulations.

2.3 Connection of state-space models

For the validation case in this paper, the outputs of the acoustic system have been chosen to be velocity perturbations u' at the flame reference positions upstream of the heat release zones. The inputs to the acoustic system are the volumetric heat-release fluctuations $\dot{q}'_V$ in these zones, which appear as a source term in Eq. (5). The $n - \tau$ flame model provides the time-lagged volumetric heat-release as a function of the velocity perturbations u' at the reference positions.

The connection of the acoustic and the flame models are accomplished using a state-space connection algorithm described in [9]. This is done by feeding back the output of the acoustic system u' to the input of the flame system and vice versa with $\dot{q}'_V$. This way, a closed loop is created and the connected model has no more in- or outputs. Due to the linearity of both acoustic and flame model, the resulting thermoacoustic model is also linear, which yields efficient computations both in time- and frequency-domain.

2.4 Calculation of eigenmodes

The connection of the acoustic and the flame model yields a state-space model, which incorporates the complete thermoacoustic dynamics. The stability of this system can be investigated by solving for the eigenmodes. For smaller systems (up to $N \sim 3 \times 10^4$), it is feasible to directly calculate all the eigenmodes of the system. Due to limitations in memory and computational effort, only some modes of interest are calculated for bigger systems. In order to solve for modes around a specific shift-frequency σ, the generalized, non-Hermitian eigenvalue problem in Eq. (10) has to be solved, where σ is the complex shift, λ is the complex eigenfrequency and $\mathbf{v}$ is the right-eigenvector [10].

$$(\mathbf{A} - \sigma\mathbf{E})^{-1}\mathbf{E}\mathbf{v} = \nu\mathbf{v} \quad \text{with} \quad \nu = \frac{1}{\lambda - \sigma} \tag{10}$$

The eigenfrequencies, which are closest to the shift, get moved close to zero. After inverting the problem, these are the eigenfrequencies ν with largest magnitude and can be found efficiently by the iterative Arnoldi algorithm. The eigenfrequencies λ of the original problem can then be computed with knowledge of the shift σ (Eq. (10)).

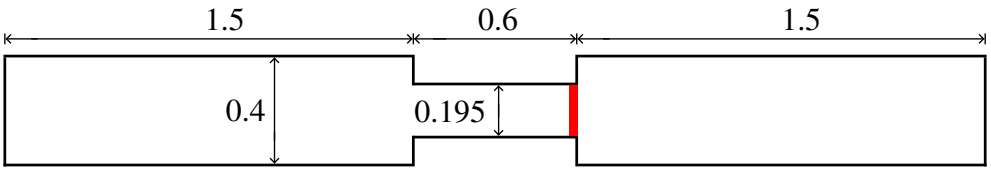

Figure 3: Annular combustor cut through one burner, all measures in m.

LU-factorizations of the stencil $(\mathbf{A} - \sigma\mathbf{E})$ are computed using the multifrontal solver MUMPS ([11], version 5.0.1), because the direct inversion would be too expensive. This factorization step takes up most of the computational time and working memory, but can be parallelized. The eigenvalue calculation is very efficient, because the matrices obtained for the state-space models of the acoustic and the FTF system are very sparse, which speeds up the vector matrix products significantly and requires little working memory. The system which was used to create the results of this paper consists of $\sim$ 203,000 states and requires $\sim$ 4 Gigabyte of RAM to solve for an eigenvalue.

3. Validation Case Setup

The capabilities of the state-space method have been validated for a well researched plenum-burner-chamber configuration [12]. This simplified model of an annular gas turbine combustion chamber consists of a plenum and a chamber of equal geometry, connected by four burner ducts, see Fig. 3 for a cross-section through one burner. The acoustic-flame interaction has been taken into account with $n - \tau$ models. Volumetric heat-release fluctuations $\dot{q}'_V$ of the flames are assumed to be localized at the burner-chamber interface in a volume which amounts to 5 % of the duct volume. The configuration has zero mean-flow velocity and exhibits a temperature jump from 700 K in the plenum and the burners to 1800 K in the chamber. Further parameters can be found in Table 1 of [12].

The numerical setup has been done in COMSOL Multiphysics. A tetrahedral spatial discretization with refinements in proximity to the heat-release areas was employed. For this mesh with $\sim$ 225,000 Elements, a state-space model with $N_A \sim$ 206,000 degrees of freedom was exported. The mesh size is similar to the AVSP mesh used in [12]. All the boundaries were modeled as hard slip-walls and linear testfunctions were used. Note that in three dimensions, each node will result in 5 degrees of freedom (p', ρ', $\mathbf{u}'$), but Dirichlet boundary conditions will eliminate some of these states.

Conversion from non-dimensional to dimensional heat-release rate fluctuations $\dot{q}'_{V,i}$ for the i-th burner (Eq. (11)) is done through incorporating a constant factor in the output-matrix $\mathbf{C}$ of the flame state-space system.

$$\dot{q}'_{V,i} = \frac{\gamma \bar{p} S_i}{\gamma - 1} n_i u'(t - \tau) \tag{11}$$

Here, γ is the ratio of specific heats, $\bar{p}$ is the mean pressure and S_i is the burner cross-section. For the mode calculation in this paper, the same n and τ were chosen for all four burners.

4. Results

Validation of this method is carried out against the results of the Finite-Volume Solver AVSP reported in [12] by comparing the azimuthal eigenmodes. Azimuthal modes appear in pairs with opposite rotational directions (clockwise and counter-clockwise), which can exhibit different eigenfrequencies. However, if the case is perfectly rotational symmetric, both modes become standing modes and coincide on the same frequency. Subsequently, these modes are called degenerate. The investigated plenum-burner-chamber configuration features coupling between the azimuthal eigenmodes of the cold plenum and the hot chamber. The strength of this coupling depends, for a given n, on the time delay τ of the flame model.

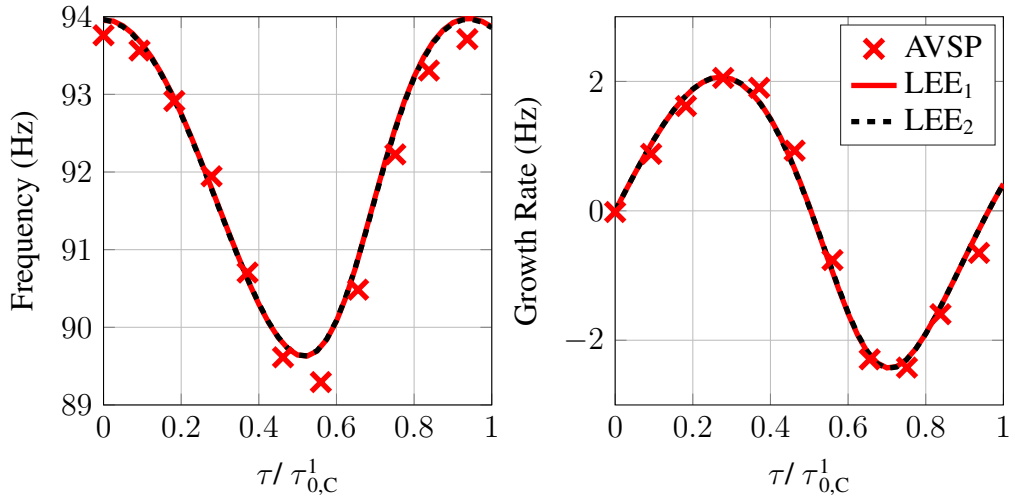

Figure 4: Eigenfrequencies and growth rates for WCC1 of the presented state-space method compared to AVSP results reported in [12].

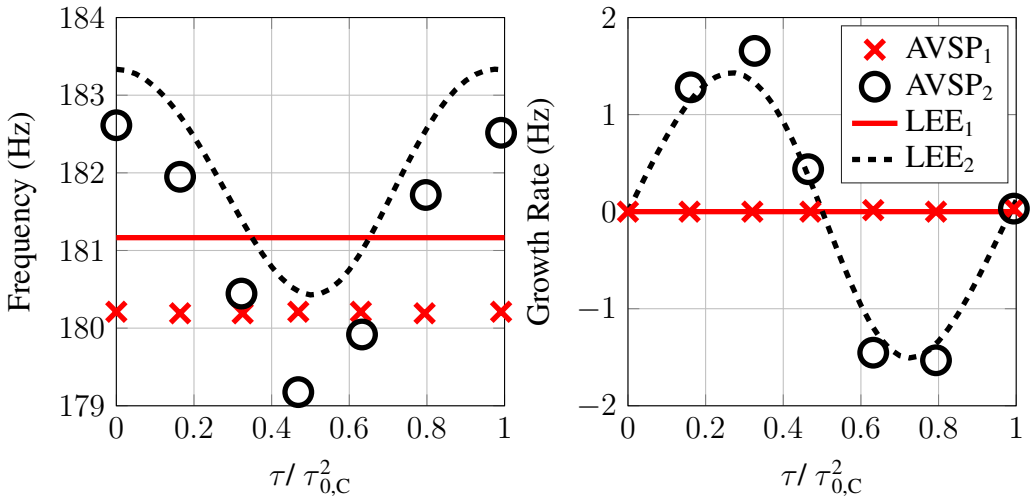

Figure 5: Eigenfrequencies and growth rates for WCC2 of the presented state-space method compared to AVSP results reported in [12].

Figures 4 and 5 show the frequencies and the growth rates of the first (WCC1) and second (WCC2) **W**eakly **C**oupled azimuthal **C**hamber modes. The indices 1 and 2 denote the first and second mode of the azimuthal mode pair. Note that τ has been non-dimensionalized by the respective decoupled chamber mode time period $\tau^1_{0,C}$ and $\tau^2_{0,C}$. The period times for the m-th chamber mode is given by Eq. (12), L_C and c^0 are the half-perimeter and the speed of sound in the chamber [12].

$$\tau^m_{0,C} = \frac{2L_C}{mc^0} \tag{12}$$

The increasing time-delay of the FTF changes the relative phase between the heat release and the acoustic velocity perturbations of the mode. For $\tau/\tau_{0,C} < 0.5$, the interference between these perturbations leads to a net increase in perturbation energy. As neither damping mechanisms nor energy loss at the domain boundaries are present, the mode becomes unstable. With further increase in τ, the shift in phase angle leads to a destructive interference between heat release and acoustic pressure, the mode stabilizes and thus exhibits negative growth-rates. Both the WCC1 and WCC2 modes show this behavior.

Very good agreement between the results of the state-space method and AVSP can be found for the WCC1 mode. The two modes are degenerate and have identical frequencies and growth-rates. For

Figure 6: WCC1 (left) and WCC2 (right) eigenmodes for $n = 1.57$ and $\tau/\tau_{0,C} = 0.5$.

the WCC2 mode frequencies, an almost constant off-set of ~ 1 Hz compared to AVSP can be found for both modes. However, the basic nature of the WCC2 modes is present in both compared models: The first WCC2 mode exhibits pressure nodes at the burners and thus doesn't excite any acoustic velocity perturbations in the burner ducts. Consequently, there is no influence of the time delay τ on this mode. The second mode (Fig. 6) right) strongly depends on the time delay of the flame due to the pressure anti-nodes at the burners.

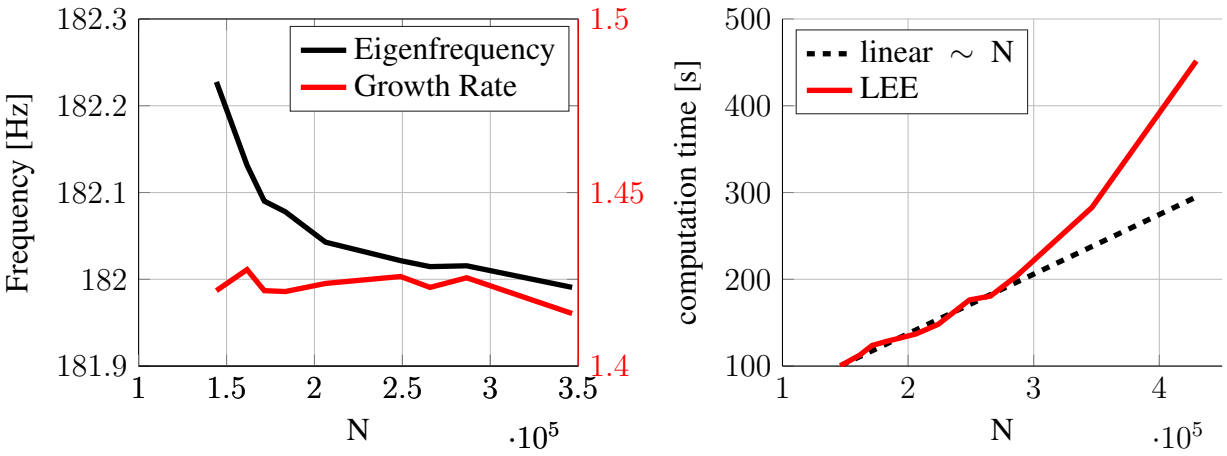

Figure 7: WCC2 eigenfrequency convergence (left, $n = 1.57$, $\tau/\tau_{0,C}^2 = 0.25$) and computation time (right) with increasing system order N.

Computational efficiency and convergence are shown in Fig. 7. As can be seen, the eigenfrequency is only slightly mesh dependent for $N > 2 \times 10^5$. For simplicity, only the WCC2 mode is shown. This convergence behavior is similar for all investigated modes and growth rates.

The computation time for the eigenmodes scales linearly for small to medium systems, then takes a superlinear trend for larger N. Notice that all the computations have been carried out on a single core of a desktop PC. It is assumed, that a better scaling for large systems can be achieved by parallel processing. The calculation of an eigenmode using AVSP takes 5 to 30 minutes on 14 cores for a mesh containing $\sim$ 57,000 cells and depends on the thermoacoustic coupling between plenum and chamber. For strong coupling, convergence is significantly slower. The same calculations for a state-space model with $\sim$ 206,000 degrees of freedom ($\sim$ 225,000 cells in the FEM discretized mesh) take around 2 minutes. The presented state space eigenvalue solver has no convergence issues depending on the mode-shape or the coupling strength and shows superior performance because, compared to AVSP, no iterations for the flame coupling are required.

5. Conclusion

The gap in terms of computational effort and complexity between (analytical) low-order models and very costly LES can be closed based on linearized acoustic equations. Following this idea, state-space models offer great efficiency and robustness when combined with very sparse system matrices, as obtained from discretized LEE or FTFs. The ability to connect these models yields a closed

description of thermoacoustic systems in complex geometries, while retaining the linear eigenvalue problem. Network models, which are based on state-space descriptions, such as taX ([9]), can be used to combine FEM models with low-order acoustic elements to increase their range of application. As shown in this paper, state-space models can make the stability analysis in complex geometries affordable.

6. Acknowledgement

We thank M. Bauerheim for his cooperation and making his results available.

REFERENCES

1. Emmert, T., Jaensch, S., Sovardi, C. and Polifke, W. taX - a Flexible Tool for Low-Order Duct Acoustic Simulation in Time and Frequency Domain, *7th Forum Acusticum*, Krakow, Sep., (2014).

2. Evesque, S. and Polifke, W. Low-Order Acoustic Modelling for Annular Combustors: Validation and Inclusion of Modal Coupling, *Int'l Gas Turbine and Aeroengine Congress & Exposition*, Amsterdam, NL, ASME GT-2002-30064, (2002).

3. Schuermans, B., Bellucci, V. and Paschereit, C. O. Thermoacoustic Modeling and Control of Multi-Burner Combustion Systems, *Int'l Gas Turbine and Aeroengine Congress & Exposition*, Atlanta, GA, U.S.A., pp. 509–519, GT2003-38688, ASME, (2003).

4. Bothien, M., Moeck, J., Lacarelle, A. and Paschereit, C. O. Time domain modelling and stability analysis of complex thermoacoustic systems, *Proceedings of the Institution of Mechanical Engineers, Part A: Journal of Power and Energy*, **221** (5), 657–668, (2007).

5. Nicoud, F., Benoit, L., Sensiau, C. and Poinsot, T. Acoustic modes in combustors with complex impedances and multidimensional active flames, *AIAA Journal*, **45** (2), 426–441, (2007).

6. Gikadi, J., *Prediction of Acoustic Modes in Combustors using Linearized Navier-Stokes Equations in Frequency Space*, Phd thesis, Technische Universität München, Garching, Germany, (2013).

7. Lieuwen, T. and Yang, V. Eds., *Combustion Instabilities in Gas Turbine Engines: Operational Experience, Fundamental Mechanisms, and Modeling*, vol. 210 of *Progress in Astronautics and Aeronautics*, AIAA (2005).

8. Subramanian, P., Blumenthal, R. S., Sujith, R. and Polifke, W. Distributed time lag response functions for the modelling of combustion dynamics, *Combustion Theory and Modelling*, **19** (2), 223–237, (2015).

9. Emmert, T., Meindl, M., Jaensch, S. and Polifke, W. Linear State Space Network Modeling of Acoustic Systems, *submitted to Acta Acustica united with Acustica*, (2016).

10. Lehoucq, R., Sorensen, D. and Yang, C., *ARPACK Users' Guide*, Software, Environments and Tools, Society for Industrial and Applied Mathematics (1998).

11. Amestoy, P. R., Duff, I. S., L'Excellent, J.-Y. and Koster, J., (2000), MUMPS: A General Purpose Distributed Memory Sparse Solver. Sørevik, T., Manne, F., Gebremedhin, A. H. and Moe, R. (Eds.), *Applied Parallel Computing. New Paradigms for HPC in Industry and Academia*, pp. 121–130, no. 1947 in Lecture Notes in Computer Science, Springer Berlin Heidelberg.

12. Bauerheim, M., Parmentier, J.-F., Salas, P., Nicoud, F. and Poinsot, T. An analytical model for azimuthal thermoacoustic modes in an annular chamber fed by an annular plenum, *Combustion and Flame*, **161** (5), 1374–1389, (2014).